

Genetic Programming for Multi-Timescale Modeling

Kumara Sastry,¹ D. D. Johnson,¹ David E. Goldberg,² Pascal Bellon¹

¹Department of Materials Science & Engineering, and the Fredrick Seitz Materials Research Laboratory.

²Department of General Engineering

University of Illinois Urbana-Champaign, Urbana IL.

(Dated: November 7, 2018)

A bottleneck for multi-timescale dynamics is the computation of the potential energy surface (PES). We explore the use of genetic programming (GP) to symbolically regress a mapping of the saddle-point barriers from only a few calculated points via molecular dynamics, thereby avoiding explicit calculation of all the barriers. The GP-regressed barrier function enables use of kinetic Monte Carlo (KMC) to simulate real-time kinetics (seconds to hours) using realistic interactions. To illustrate, we apply a GP regression to vacancy-assisted migration on a surface of a binary alloy and predict the diffusion barriers within 0.1–1% error using 3% (or less) of the barriers, and discuss the significant reduction in CPU time.

PACS numbers: 02.60.-x, 02.70.Wz, 31.50.-x, 68.35.Fx

Molecular dynamics (MD) is extensively used for kinetic modeling of materials. Yet MD methods are limited to nanoseconds of real time, and hence fail to model directly many processes. Recently several approaches were proposed for multiscale [1, 2, 3, 4, 5, 6, 7, 8, 9, 10, 11]. Methods such as temperature-accelerated dynamics (TAD) [2] provide significant acceleration of MD but they still fall 3–6 orders of magnitude short of real processing times. These methods assume that transition-state theory applies, and concentrate only on infrequent events. An alternative approach to bridge timescales [4] uses kinetic Monte Carlo (KMC) [12] combined with MD by constructing an *a priori* list of events (i.e., “look-up table”). The table look-up KMC yields several orders of magnitude increase in *simulated* time over MD (e.g., see [22]). The table of events is commonly comprised of atomic jumps, but collective motions (or off-lattice jumps), e.g., see [7], may need to be added but may not be known *a priori*. Additionally, tabulating barrier energies from a list of events is a serious limitation. For example, multicomponent alloys have an impossibly large set of barriers, due to configurational dependence, making their tabulation impractical, especially from first-principles. An alternative approach is calculating energies “on-the-fly” [6, 13], but it too has serious time limitation (see Fig. 1). Recent developments and limitations of KMC methods are given, e.g., in [13].

Symbolically-Regressed Table KMC (sr-KMC): To avoid the need or expense of explicit calculation of all activation barriers—frequent or infrequent—and thereby facilitate an effective hybridization of MD and KMC for multiscale dynamics modeling, we utilize genetic programming (GP)—a genetic algorithm that evolves computer programs—to symbolically regress the PES (in our case saddle-point barriers only) from a limited set of calculated points on the PES. An accurate GP-regressed PES extends the KMC paradigm, as suggested in Fig. 1, to machine learn the “look-up table” and get an in-line

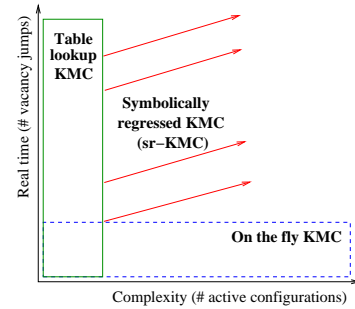


FIG. 1: Schematic illustration of simulation capabilities and bottlenecks of on-the-fly KMC, table look-up KMC, and symbolically-regressed KMC (sr-KMC).

barrier function for increasing number of active configurations (or complexity) and providing simulation over experimentally relevant time frames, which may not be possible from standard table look-up or on-the-fly KMC. Interfacing GP with TAD-MD and/or pattern-recognition methods will further extend its applicability, e.g., by finding system-specific mechanisms. Of course, sr-KMC benefits from any advances in KMC methods. In addition, GP-based symbolic regression holds promise in other multiscale areas, e.g., regressing constitutive rules and chemical reaction pathways, which we are studying. Also, as we exemplify, standard basis-set regression are generally not competitive to GP for fixed accuracy due to the difficulty in choosing appropriate basis functions.

To demonstrate, we discuss GP and its application to a non-trivial case of vacancy-assisted migration on (100) surface of phase-separating $\text{Cu}_x\text{Co}_{1-x}$. Although there are millions of configurations, only the environmental atoms locally around vacancy and migrating atom significantly influence the barrier energies. We refer to these as the *active* configurations. The results show that GP predicts barriers within 0.1–1% error using calculated barriers of less than 3% of the total *active* configura-

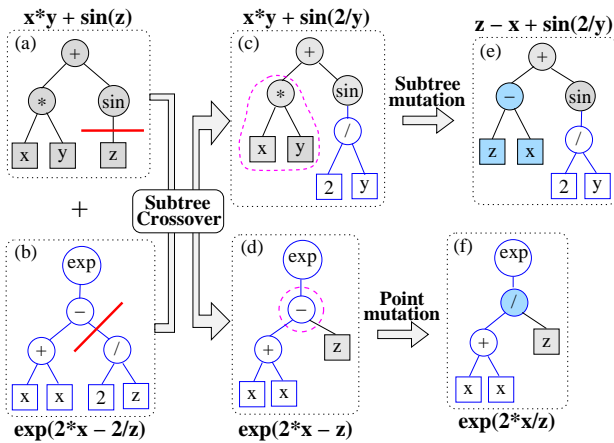


FIG. 2: Illustration of tree representation, subtree crossover, subtree mutation, and point mutation used in GP.

tions. For alloys, this technique can be combined with a local cluster expansion technique [14] that reduces the explicit barrier calculations to $\sim 0.3\%$ of the *active* configurations. Our initial results hold promise to enable the use of KMC (even with realistic potentials) for increased problem complexity with a scale-up of simulation time.

Genetic programming [15] is a genetic algorithm that evolves computer programs. The program is represented by a tree consisting of functions in the internal nodes and terminals in the leaf nodes (Fig. 2a). Here we use the function set $\mathcal{F} = \{+, -, *, /, \wedge, \exp, \sin\}$ and the terminal set $\mathcal{T} = \{\vec{x}, \mathcal{R}\}$, where \vec{x} is a vector representing the *active* alloy configuration, and \mathcal{R} is an ephemeral random constant [15]. Since we use GP for predicting the barriers, a tree represents a PES-prediction function that takes a configuration and ephemeral constants as inputs and returns the barrier for that configuration as output.

A tree's quality is given by its fitness f . For this, we calculate the barriers $\{\Delta E_{\text{calc}}(\vec{x}_1), \dots, \Delta E_{\text{calc}}(\vec{x}_M)\}$ for M random configurations $\{\vec{x}_1, \vec{x}_2, \dots, \vec{x}_M\}$. These configurations are used as inputs to the tree and the barriers $\{\Delta E_{\text{pred}}(\vec{x}_1), \dots, \Delta E_{\text{pred}}(\vec{x}_M)\}$, are predicted. The fitness is then computed as a weighted average of the absolute error between the predicted and calculated barriers:

$$f = \frac{1}{M} \sum_{i=1}^M w_i |\Delta E_{\text{pred}}(\vec{x}_i) - \Delta E_{\text{calc}}(\vec{x}_i)| \quad (1)$$

with $w_i = |\Delta E_{\text{calc}}|^{-1}$, which gives preference to accurately predicting lower energy (most significant) events.

Unlike traditional search methods, GP uses a population of candidate solutions (PES prediction functions) that are initially created using the *ramped half-and-half* method [15]. Once the population is initialized and evaluated, the following genetic operators are repeatedly applied till one or more convergence criteria are satisfied:

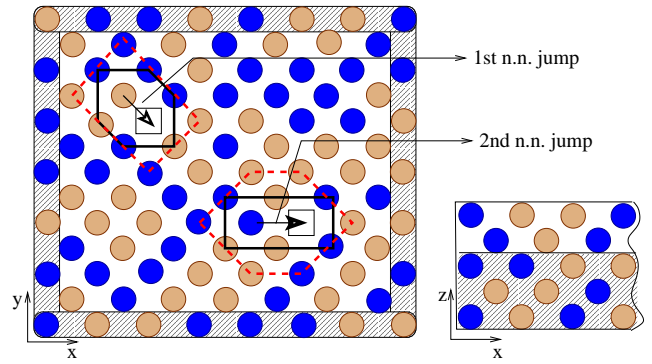


FIG. 3: Sketch of simulation cell for vacancy-assisted migration on (100)-surface of an fcc binary alloy. Atoms in all but the bottom layers and the boundary can fully relax. The solid (dashed) lines around the migrating atom and vacancy represent 1st (2nd) n.n. environmental atoms.

Selection: allocates more copies to solutions with better fitness values. We use an *s-wise tournament selection* [16], where s candidate solutions are randomly chosen and pitted against each other in a tournament. A solution with the best fitness wins.

Recombination combines bits and pieces of two solutions to create new, hopefully better, solutions. We use *subtree crossover* [15], where a crossover point for each solution is randomly chosen and subtrees below the point are swapped to create two new solutions, see Fig. 2.

Mutation locally but randomly modifies a solution. We use two mutation techniques (see Fig. 2): *Subtree mutation*, where a subtree is randomly replaced with another randomly created subtree, and *point mutation* where a node is randomly modified.

Case Study: We consider the prediction of diffusion barriers for vacancy-assisted migration on (100) surface of phase-separating $\text{Cu}_x\text{Co}_{1-x}$. The system consists of five layers with 100 to 625 atoms in each layer (see Fig. 3). The bottom three layers are held fixed to their bulk bond distances, while the top layers are either held fixed (as a test) or fully relaxed via MD. We consider only first and second nearest-neighbor (n.n.) jumps, along with 1st (as a test) and 2nd n.n. environmental atoms in the active configuration, as shown in Fig. 3. This system already exhibits large complexity and is still small enough so that table look-up and GP-regressed KMC can be implemented and directly compared. Table I gives the number of active configurations when 1st and 2nd n.n. environments are considered for a binary alloy.

We model the atomic interactions with a simple Morse potential [17] and a tight-binding potential with second-moment approximation (TB-SMA) [18]. To validate interactions, we model vacancy-assisted migration on (100)-surface of Cu and consider only first n.n. jumps. The predicted barrier for n.n. vacancy jumps with fully relaxed lattice in Cu is 0.39 eV for Morse and 0.45 eV

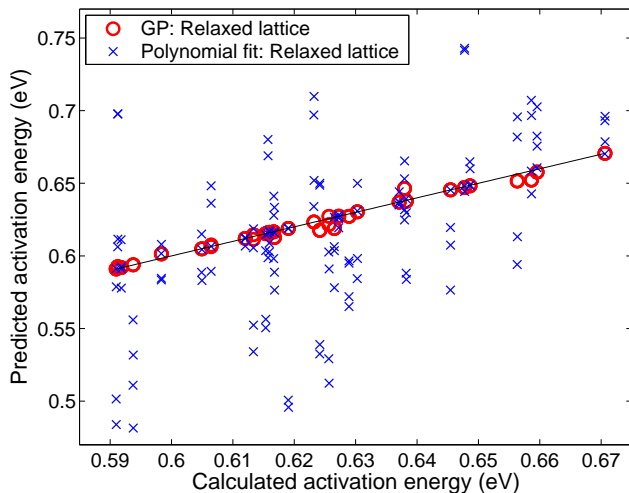


FIG. 4: Activation energies (in eV) predicted by regression. GP (circles) and a quadratic polynomial (crosses) are compared to the calculated (Morse) barriers for 1st n.n. jumps on (100)-surface of $\text{Cu}_{0.5}\text{Co}_{0.5}$ for relaxed lattices. As a simple test, only first n.n. environments are considered in the active configuration. The line is a guide for the eye.

for TB-SMA, agreeing with 0.42 ± 0.08 (0.47 ± 0.05) from *ab initio* (EAM) [19] calculations.

We now consider the barrier regression via GP for vacancy-assisted migration on (100)-surface of $\text{Cu}_x\text{Co}_{1-x}$. The input to the barrier regression (i.e., prediction) function, $\vec{x} = \{x_j\}$ is a binary-encoded vector sequence, where $x_j = 0$ (1) represents a Cu (Co) atom. For simplicity, we begin by considering only seven 1st n.n. environmental atoms yielding 128 *active* configurations. About 20, i.e., 16%, different active configurations are randomly chosen and their barriers are computed using the conjugate-gradient method and are used in the GP fitness function, see Eq. 1. The barriers predicted by GP for the relaxed configurations are compared to the exact values in Fig. 4. We note that the prediction error for rigid lattice case ($0.4 \pm 0.04\%$) is significantly less than that for relaxed lattice case ($2.8 \pm 0.08\%$). Due to the weighting used in the fitness function, GP predicts barriers for most significant events more accurately than for less-significant (higher-energy) events.

Figure 4 also compares the barriers predicted by GP to those predicted by a least-squares fit quadratic polynomial, showing clearly its inadequacy for alloys. Further-

TABLE I: Number of active configurations for 1st and 2nd n.n. jumps, and for 1st and 2nd n.n. active atoms

	1 st n.n. jumps	2 nd n.n. jumps
1 st n.n. active configurations	128	128
2 nd n.n. active configurations	2048	8192
Total configurations	$\gg 2^{100}$	$\gg 2^{100}$

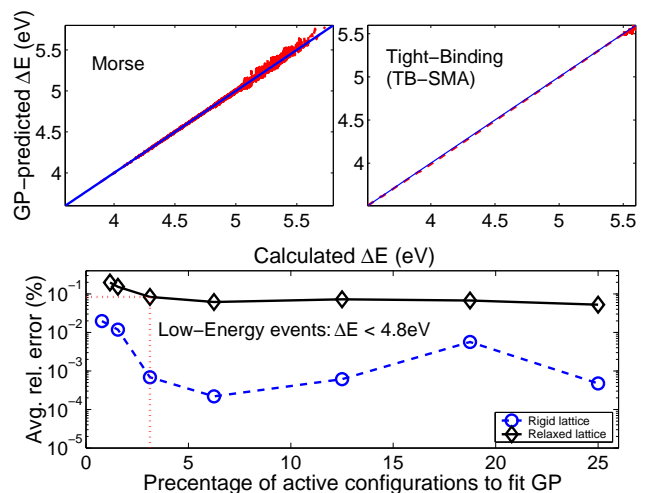


FIG. 5: (Upper) Calculated vs. GP-predicted barriers (in eV) for 2nd n.n. jumps on relaxed (100)-surface of $\text{Cu}_{0.5}\text{Co}_{0.5}$ active configurations up to 2nd n.n. for Morse and TB-SMA. (Lower) GP predicts the barriers with 0.1% (1%) error for most- (less-) significant events with $\Delta E < 4.8$ eV ($\Delta E > 4.8$ eV) from only 3% of active configurations.

more, while GP requires only 16%, the quadratic (cubic) polynomial fit needs 27% (78%) of the barriers. In limited cases, such as dilute $\text{Fe}_{1-x}\text{Cu}_x$, the barriers can be predicted via a simple polynomial fit [20].

To test the scalability of GP with *active* configuration size, we consider the 2nd n.n. jumps and 1st and 2nd n.n. environmental atoms in the *active* configuration. As shown in Table I, there are a total of 8192 configurations. The energies predicted by GP are compared with direct calculations in Fig. 5, along with the error. The GP predicts the barriers for most significant events with less than 0.1% error by fitting to energies from only 3% (i.e., 256/8192) of the active configurations (with error defined in [23]). In comparison, a cubic polynomial fit requires energies for $\sim 6\%$ of the configurations, predicting the barriers with 2.5% error for the most significant events.

The results shown in Figs. 4 and 5 clearly demonstrate the effectiveness of GP in predicting the potential energy surface, with high accuracy and little information. As expected, since the regression and barrier calculation are nearly independent, the GP performance does not depend on the potentials used, e.g., Fig. 5 shows results for both Morse, and non-additive and non-linear tight-binding potentials. The regression only requires a database of barriers and has no knowledge (nor the need) of the underlying potential used. We also find that the GP performance is independent of the configuration set used in calculating the fitness function, the order in which they are used, and the labeling scheme used to convert the configuration into a vector of inputs. Differences in activation-energy scale on the PES prediction via GP is also negligible. That is, even though the barriers for the

1st and 2nd n.n. jumps differ by an order of magnitude, GP predicts the barriers with similar accuracy. Moreover, for more complex, cooperative effects, such as island diffusion via surface dislocations [21], sr-KMC could be interfaced with pattern-recognition methods [24] (see [25] for long-range fields).

Time enhancements by coupling a GP-regressed barriers with KMC (or sr-KMC) are simple to estimate. For our example, with ~ 33 times fewer calculated barriers GP symbolically regresses an in-line barrier function—rather than the complete look-up table—and thus, sr-KMC provides a direct CPU savings of ~ 100 over table look-up methods. Additionally, each time step of sr-KMC requires only 10^{-3} CPU-seconds for an in-line function evaluation, as opposed to on-the-fly KMC which require seconds (empirical potentials) to hours (quantum methods), thus providing a gain of 10^4 – 10^7 CPU-seconds. For our example, one relaxed barrier calculation takes ~ 10 secs (~ 1800 secs) for Morse (TB-SMA). One important question, especially for bulk diffusion, is how the gain from sr-KMC scales with system complexity. While we cannot fully answer this question yet, in the present study it is remarkable and promising that the fraction of explicit barrier calculations required by sr-KMC decreases as the number of active configurations increases.

To summarize, potential energy surface prediction using symbolic regression via genetic programming (GP) holds promise as an efficient tool for multi-scaling in dynamics. The GP based KMC approach avoids the need or expense of calculating the entire potential-energy surface, is highly accurate, and leads to significant scale-up in simulation time and a reduction in CPU time. We have shown on a non-trivial example of vacancy-assisted migration on a surface of $\text{Cu}_x\text{Co}_{1-x}$ that GP predicts all barriers with 0.1–1% error from calculations for only 3% of active configurations, allowing seconds of simulation time. For alloy problems, the number of direct barrier calculations can further be reduced by over an order of magnitude by hybridizing GP with cluster expansion methods [14]. We emphasize that the GP is non-trivially regressing a function and its coefficients that approximates the potential-energy surface, and its efficacy over standard basis-set regression is clear. Moreover, GP approach is not problem specific and requires little modification, if any (say by choice of operators and functions), to address increasingly complex cases, and as suggested, is potentially useful in other multiscaling areas.

This work was supported by the NSF at Materials Computation Center (ITR grant DMR-99-76550), CPSD (ITR grant DMR-0121695), AFOSR (grant F49620-00-0163), Computational Science & Engineering fellowship and the Dept. of Energy through the Fredrick Seitz MRL (grant DEFG02-91ER45439) at UIUC. We gratefully ac-

knowledge discussions with R.S. Averback, Y. Ashkenazy, and J.-M. Roussel.

-
- [1] A. F. Voter, Phys. Rev. Lett. **78**, 3908 (1997).
 - [2] A. F. Voter, Phys. Rev. B **57**, R13985 (1998).
 - [3] A. F. Voter, F. Montalenti, and T. C. Germann, Annu. Rev. Mater. Res. **32**, 321 (2002).
 - [4] J. Jacobsen, B. H. Cooper, and J. P. Sethna, Phys. Rev. B **58**, 15847 (1998).
 - [5] T. Diaz De La Rubia et al., J. Comp.-Aided Mat. Design **5**, 243 (1998).
 - [6] G. Henkelman and H. Jónsson, J. Chem. Phys. **111**, 7010 (1999), *ibid* **113**, 9978 (2000); *ibid* **115**, 9657 (2001).
 - [7] M. R. Sørensen and A. F. Voter, J. Chem. Phys. **112**, 9599 (2000).
 - [8] W. Cai, M. H. Kalos, M. de Koning, and V. V. Bulatov, Phys. Rev. E **66**, 046703 (2002).
 - [9] M. M. Steiner and P.-A. Genilloud, Phys. Rev. B **57**, 10236 (1998).
 - [10] G. T. Barkema and N. Mousseau, Phys. Rev. Lett. **77**, 4358 (1996).
 - [11] G. T. Barkema and N. Mousseau, Comput. Mat. Sc. **20**, 285 (2001).
 - [12] K. Binder, ed., *Monte Carlo methods in statistical physics* (Springer, Berlin, 1986).
 - [13] J. L. Bocquet, Defect and Diffusion Forum **203–205**, 81 (2002).
 - [14] A. Van der Ven and G. Ceder, Phys. Rev. B **64**, 184307 (2001).
 - [15] J. R. Koza, *Genetic programming: On the programming of computers by means of natural selection* (MIT Press, Cambridge, MA, 1992).
 - [16] D. E. Goldberg, B. Korb, and K. Deb, Complex Systems **3**, 493 (1989).
 - [17] L. Girifalco and V. Weizer, Phys. Rev. **114**, 687 (1959).
 - [18] N. Levano et al., Phys. Rev. B **61**, 2230 (2000).
 - [19] G. Boisvert and L. Lewis, Phys. Rev. B **56**, 7643 (1997).
 - [20] Y. L. Bouar and F. Soisson, Phys. Rev. B **65**, 094103 (2002).
 - [21] J. C. Hamilton, M. S. Daw, and S. M. Foiles, Phys. Rev. Lett. **74**, 2760 (1995).
 - [22] For Cu-Co $\nu_o \approx 27 \times 10^{12}$ Hz [19], giving per time step of KMC relative to MD (assuming an MD time-step of 10^{-15} s) 10^9 increase in *simulated* time over MD at 300 K, 10^4 at 650 K, and $10^{2.3}$ at 1000 K
 - [23] The average relative error for N'_{cfgs} configurations within the desired energy range is given by

$$\bar{\epsilon}_{\text{rel}} = \frac{100}{N'_{\text{cfgs}}} \sum_{i=1}^{N'_{\text{cfgs}}} \left| \frac{\Delta E_{\text{pred}}(\vec{x}_i) - \Delta E_{\text{calc}}(\vec{x}_i)}{\Delta E_{\text{calc}}(\vec{x}_i)} \right|,$$

- [24] Talat Rahman, private communication
- [25] For long-range fields (e.g., elastic fields from coherent interfaces, such as multilayers or precipitates), a description based solely on local configurations may have to be extended, say, with phase field methods.

